Cancer Cell
Article

CRL4B Catalyzes H2AK119 Monoubiquitination and Coordinates with PRC2 to Promote Tumorigenesis

Huili Hu,[1] Yang Yang,[1] Qinghong Ji,[1] Wei Zhao,[1] Baichun Jiang,[1] Ruiqiong Liu,[1] Jupeng Yuan,[1] Qiao Liu,[1] Xi Li,[1] Yongxin Zou,[1] Changshun Shao,[1] Yongfeng Shang,[2] Yan Wang,[1,2,*] and Yaoqin Gong[1,*]
[1]Key Laboratory of Experimental Teratology, Ministry of Education, Institute of Molecular Medicine and Genetics, Shandong University School of Medicine, Jinan, Shandong 250012, China
[2]2011 Collaborative Innovation Center of Tianjin for Medical Epigenetics, Tianjin Key Laboratory of Medical Epigenetics, Department of Biochemistry and Molecular Biology, Tianjin Medical University, Tianjin 300070, China
*Correspondence: yanwang@tmu.edu.cn (Y.W.), yxg8@sdu.edu.cn (Y.G.)
http://dx.doi.org/10.1016/j.ccr.2012.10.024

SUMMARY

We reported that Cullin4B-Ring E3 ligase complex (CRL4B) is physically associated with Polycomb-repressive complex 2 (PRC2). We showed that CRL4B possesses an intrinsic transcription repressive activity by promoting H2AK119 monoubiquitination. Ablation of *Cul4b* or depletion of CUL4B, the main component of CRL4B, resulted in loss of not only H2AK119 monoubiquitination but also H3K27 trimethylation, leading to derepression of target genes that are critically involved in cell growth and migration. We demonstrated that CUL4B promotes cell proliferation, invasion, and tumorigenesis in vitro and in vivo and found that its expression is markedly upregulated in various human cancers. Our data indicate that CUL4B promotes tumorigenesis, supporting the pursuit of CUL4B as a target for cancer therapy.

INTRODUCTION

Compared to other histone modifications, ubiquitination represents a very large modification and is mainly found on H2A lysine 119 (K119) and H2B (K120 in human and K123 in yeast) (Kouzarides, 2007). Polycomb group proteins are a family of epigenetic regulators responsible for the repression of an array of genes that are critically implicated in development and cell fate specification (Schuettengruber et al., 2007). Two main Polycomb group complexes exist in mammals: PRC1 and PRC2. PRC1 catalyzes histone H2A K119 monoubiquitylation (H2AK119ub1) and compacts chromatin (Wang et al., 2004), while PRC2 catalyzes trimethylation of histone H3 at K27 (H3K27me3) and also contributes to chromatin compaction (Simon and Kingston, 2009). It is believed that PRC1 and PRC2 interplay and that H2AK119ub1 and H3K27me3 are functionally coordinated in transcriptional repression (Müller and Verrijzer, 2009). Although this premise is still cited in the literature, its operational status is equivocal as there are genes that are targeted by PRC2 without PRC1, and vice versa (Tavares et al., 2012). Clearly, there is still much to be learned about the molecular mechanism underlying the coordination between H2AK119ub1 and H3K27me3.

Cullin 4-Ring E3 ligases (CRL4), assembled with CUL4, DDB1, and ROC1 as the core components, participate in a broad variety of physiologically and developmentally controlled processes such as cell cycle progression, replication, and DNA damage response (Jackson and Xiong, 2009). In mammals, there are two Cullin 4 members, CUL4A and CUL4B. Loss-of-function mutation in the X-linked *CUL4B* causes mental retardation, short statue, absence of speech, and other phenotypes in humans (Zou et al., 2007). In *CUL4B* heterozygotes, the cells in which wild-type (WT) *CUL4B* allele is inactivated are severely selected against, underscoring the functional importance of CUL4B in cellular proliferation (Zou et al., 2007). Accordingly, *Cul4b* knockout mice are embryonically lethal (Jiang et al., 2012). It is interesting that CUL4B, unlike CUL4A and other Cullins, carries a nuclear localization signal (NLS) in its N terminus and is also localized in the nucleus (Nakagawa and Xiong, 2011; Zou et al., 2009), suggesting that CUL4B might be involved in the nucleus-based functions. We addressed these issues using molecular, cellular, and epigenetic approaches plus animal models.

Significance

Cullin 4B (CUL4B) is a scaffold protein of the Cullin4B-Ring E3 ligase complex (CRL4B) that functions in proteolysis. However, recent studies indicate that CUL4B could also be localized in the nucleus, suggesting that CUL4B might be also involved in the nucleus-based functions. In addition, although it was shown that H2AK119 monoubiquitination plays a central role in transcriptional repression by coordinating with H3K27 trimethylation, the underlying mechanisms remains to be clarified. We demonstrated CRL4B is an alternative histone modification enzyme responsible for H2AK119ub1 and that CRL4B and PRC1 bind to PRC2 subunits in a mutually exclusive manner. These data provide a molecular basis for the functional interplay between H2AK119ub1 and H3K27me3 in transcription repression.

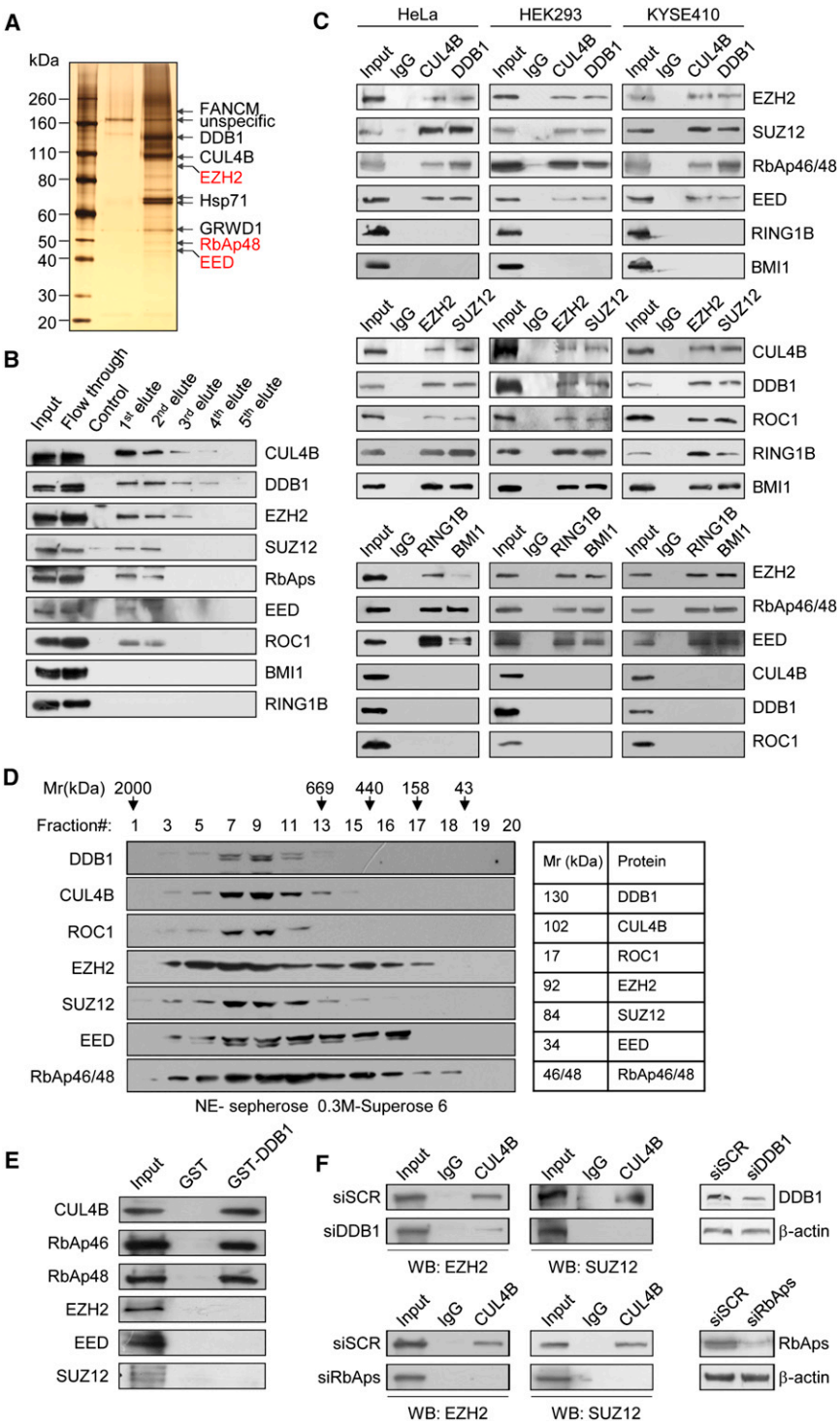

Figure 1. CRL4B Interacts with PRC2

(A) Immunoaffinity purification of CUL4B-containing protein complexes. Cellular extracts from HeLa cells stably expressing FLAG (control) or FLAG-CUL4B were immunopurified with anti-FLAG affinity columns and eluted with FLAG peptide. The eluates were resolved by SDS-PAGE and silver-stained. The protein bands were retrieved and analyzed by mass spectrometry. Detailed results from the mass spectrometric analysis are provided as Table S1.

(B) Western blotting analysis of the purified fractions using antibodies against the indicated proteins.

(C) Association of CRL4B with PRC2 in HeLa, HEK293, and KYSE410 cells. Whole cell lysates were immunoprecipitated with the antibodies against the indicated proteins. Immunocomplexes were then immunoblotted using antibodies against the indicated proteins. IgG served as the negative control.

(D) Cofractionation of the CRL4B complex and the PRC2 complex by fast protein liquid chromatography. Nuclear extracts of HeLa cells were fractionated on a DEAE sepharose column followed by a Superose 6 gel filtration column. The fractions were analyzed by western blotting. Molecular weight standards are shown on top (in kDa). The predicted molecular size of each main component of the CRL4B-PRC2 complex is summarized on the right.

(E) Molecular interaction between DDB1 and PRC2 subunits. GST pull-down experiments with bacterially expressed GST-DDB1 and the in-vitro-transcribed/translated indicated proteins.

(F) IP assays using lysates from HeLa cells transiently expressing DDB1 siRNA or RbAp48 siRNA showing decreased co-IP of CUL4B with EZH2 and SUZ12. The protein expression in these experiments was examined by western blotting using antibodies against the indicated proteins. See also Table S1.

RESULTS

Cullin 4B-RING E3 Ligase Is Physically Associated with PRC2 In Vivo

In an effort to better understand the mechanistic role of CUL4B, we used affinity purification and mass spectrometry to identify the proteins that are associated with CUL4B in vivo. In these experiments, FLAG-tagged CUL4B (FLAG-CUL4B) was stably expressed in HeLa cells. Cellular extracts were prepared and subjected to affinity purification using an anti-FLAG affinity gel. Mass spectrometric analysis indicates that CUL4B copurified with DDB1, GRWD1, COPS3, COPS4, and COPS5, as reported previously (Groisman et al., 2003; Higa et al., 2006). It is interesting that we found that CUL4B also copurified with EZH2, EED, and RbAp48, all of which are the core components of the PRC2 complex (Figure 1A). In addition, heat shock 70 kDa protein 8 (HSP71/73) and Fanconi anemia complementation group M (FANCM) were also detected in the immunocomplex. However, BMI and RING1B, the core components of PRC1 (Cao et al., 2005), did not copurify with CUL4B (Figure 1B, bottom two panels), suggesting that the association of CUL4B with PRC2 is specific. The presence of

EZH2, EED, and RbAp48 in the CUL4B-interacting complex was further confirmed by western blotting analysis (Figure 1B). The detailed results of the mass spectrometric analysis are provided in Table S1 (available online).

To further validate the in vivo interaction between Cullin 4B-RING E3 ligase (CRL4B) and PRC1/2, total proteins from HeLa cells, HEK293 cells (a human embryonic kidney cell line), and KYSE410 cells (a human esophageal squamous cell carcinoma cell line) were extracted and coimmunoprecipitation (co-IP) experiments were performed with antibodies detecting the endogenous proteins. Immunoprecipitation (IP) with antibodies against CUL4B or DDB1 followed by immunoblotting (IB) with antibodies against EZH2, SUZ12, EED, or RbAp46/48 representing PRC2 or against RING1B or BMI representing PRC1 demonstrated that only the PRC2 core components were efficiently coimmunoprecipitated with CUL4B and DDB1 (Figure 1C, upper panels). Reciprocally, IP with antibodies against EZH2 or SUZ12 followed by IB with antibodies against CRL4B subunits CUL4B, DDB1, or ROC1 or against the two PRC1 core components in these three cell lines revealed that both PRC1 and CRL4B complexes were coimmunoprecipitated with PRC2 (Figure 1C, middle panels). However, only PRC2 components could be copurified with PRC1 (Figure 1C, lower panels). These results suggest that CRL4B and PRC1 proteins bind with PRC2 components in a mutually exclusive manner.

To further support the observation that CRL4B complex is associated with PRC2 in vivo, protein fractionation experiments were carried out with nuclear proteins by fast protein liquid chromatography (FPLC). Nuclear extracts derived from HeLa cells were fractionated by DEAE sepharose, followed by superpose 6 gel filtration chromatography. Western blotting revealed a major peak at about 669-1000 kDa for CUL4B, DDB1, and ROC1, and also for PRC2 core components EZH2, SUZ12, EED, and RbAp46/48 (Figure 1D). Significantly, the chromatographic profiles of CUL4B, DDB1, and ROC1 were largely overlapped with that of the components of PRC2, supporting the argument that CRL4B complex is associated with PRC2 in vivo.

In order to further strengthen the argument, we next investigated the molecular basis for the interaction between the CRL4B complex and PRC2. For this purpose, GST pull-down assays were performed using GST-fused CUL4B or GST-fused DDB1 and in-vitro-transcribed/translated EZH2, SUZ12, EED, RbAp46, and RbAp48. These experiments revealed that, although CUL4B interacts directly with DDB1, it did not interact with the PRC2 components that we tested. However, it was shown that DDB1 could interact directly with the two DWD motif (DDB1-binding WD40 protein)-containing molecules, RbAp46 and RbAp48 (Figure 1E), suggesting that DDB1 and RbAp46/48 could act as the bridge molecules in physically linking the CRL4B complex and PRC2. It is interesting that the EED component of PRC2, which also contains a WD40 motif but has no DWD motif, did not show a direct interaction with DDB1, consistent with a previous report (He et al., 2006). The in vitro GST pull-down results were further substantiated by in vivo co-IP experiments in which depletion of either DDB1 or RbAp46/48 could disrupt the interaction between CUL4B and the PRC2 subunits, EZH2 and SUZ12, in HeLa cells (Figure 1F). Taken together, these results provide strong support for a physical association between CRL4B and PRC2 that is bridged by DDB1 and RbAp46/48.

CRL4B Exhibits Transcription Repressive Activity and Promotes H2AK119 Monoubiquitination

The physical association between CRL4B and PRC2 prompted us to investigate the hypothesis that CRL4B might be functionally involved in transcription repression. To this end, we fused CUL4B to Gal4 DNA-binding domain (Gal4-CUL4B) and tested the effect of this construct on the expression of a luciferase reporter gene driven by TK (thymidine kinase) promoter plus five copies of Gal4 binding sequence (Gal4-Luc) in HeLa cells (Figure 2A, upper panel). The results revealed that the expression of Gal4-CUL4B, but not FLAG-CUL4B, led to a drastic decrease in the expression of the reporter gene (Figure 2A, lower panel), indicating that CUL4B has an intrinsic transcriptional repression activity and suggesting that CUL4B could act as a transcription corepressor.

In order to further support this proposition, we investigated the contribution of each of the different domains of CUL4B to its transcriptional repressive function. A series of Gal4-DBD-fused deletion constructs were generated, and the repressor activities of those constructs were monitored using Gal4 UAS luciferase reporter assays (Figure 2B, upper panel). Notably, deletion of the NLS (1–137 amino acids [aa]) (ΔNLS) or NEDD8 neddylation domain (824–895 aa) (ΔNEDD8) did not affect their repressive activities, whereas deletion of either the DID (DDB1-interacting domain) region (137–287 aa) (ΔDID) or Cullin domain (578–718 aa) (ΔCullin) or both resulted in a significant reduction of the transcriptional repressive activity of CUL4B (Figure 2B, lower panel). Thus, it appears that both DID and Cullin domains are required for the transcriptional repressive activity of CUL4B, suggesting that the interaction with DDB1 and ubiquitination function of CUL4B are indispensable for its transcription repressive function.

To further explore the functional connection between CUL4B and PRC2, we performed loss-of-function experiments in the Gal4 UAS luciferase reporter system. As shown in Figure 2C, knockdown of DDB1, EZH2, or RbAps, the components of PRC2, led to a significant reduction of the transcriptional repressive activity of CUL4B, while depletion of BMI or RING1B, the core components of PRC1, had little effect. Again, these experiments suggested that CUL4B functions in transcriptional repression in the context of CRL4B and supported our hypothesis that CRL4B and PRC2 are functionally connected.

H2AK119 monoubiquitination was reported to play a central role in transcriptional repression by coordinating with H3K27me3 (Baarends et al., 2005; Müller and Verrijzer, 2009). Based on our observations that CRL4B and PRC2 are physically and functionally connected, we thus wanted to know whether CRL4B exerts transcriptional repressive activity through H2AK119 monoubiquitination. For this purpose, we performed quantitative chromatin IP (qChIP) assay in HeLa cells that were stably expressing Gal4-UAS reporter (HeLa-Gal4-Luc) to investigate the recruitment of DDB1 and EZH2 to and the changes of H2AK119ub1, H3K27me3, and H3K4me3 on the Gal4 promoter after transfection of these cells with Gal4-CUL4B or control Gal4-DBD. The results showed that artificial recruitment of CUL4B resulted in the recruitment of DDB1 and EZH2,

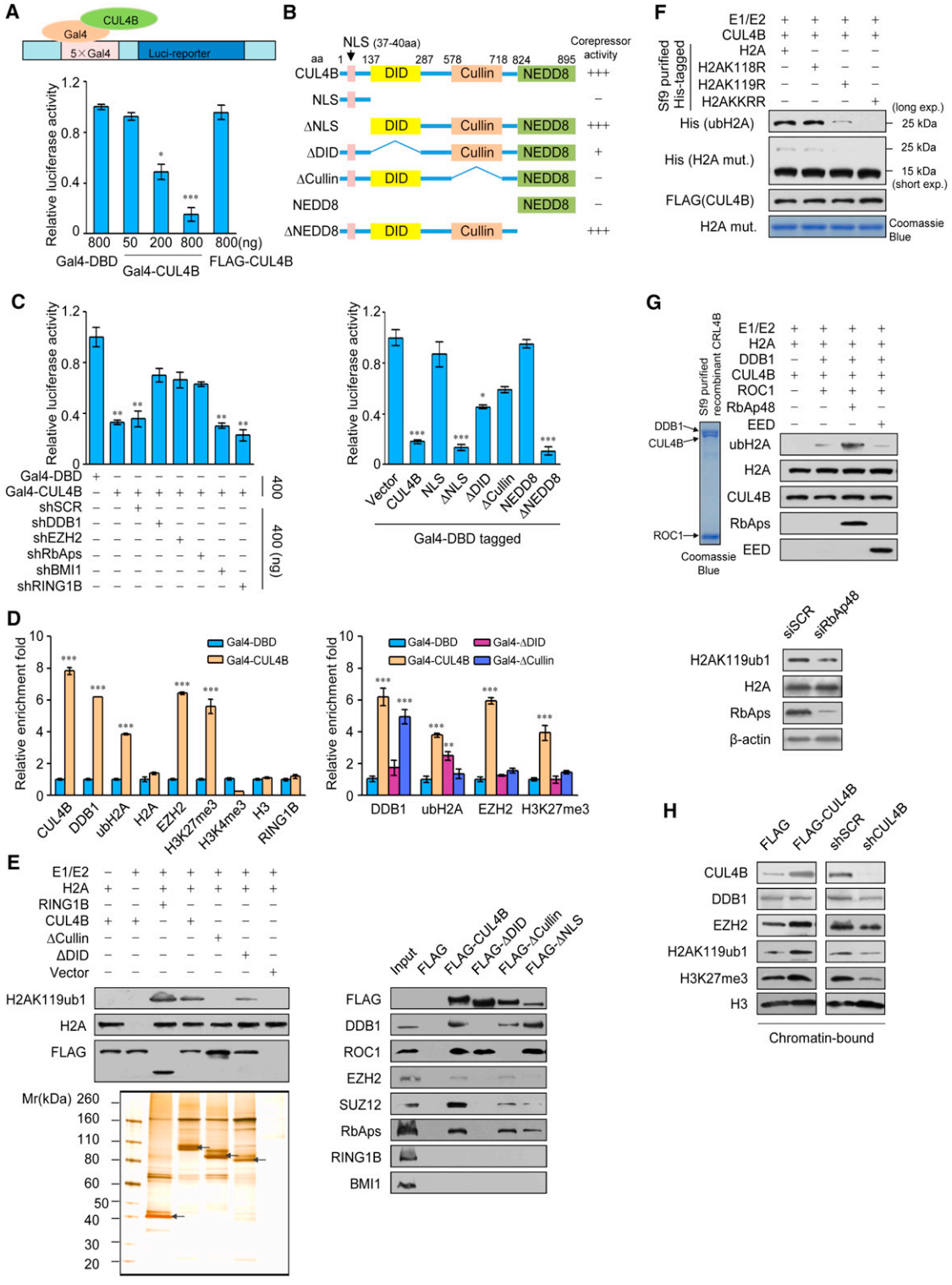

Figure 2. CUL4B Requires Its DID Domain and Cullin Domain for Optimal Repressive Activity

(A) CUL4B possesses an intrinsic transcription repressive activity. Gal4-CUL4B construct or a control vector (containing Gal4-DBD only) was transfected into HeLa cells stably expressing Gal4-UAS reporter (HeLa-Gal4-Luc cells). Gal4 luciferase reporter activity was measured.

(B) Identification of the essential domains required for the transcriptional repressive activity of CUL4B. The upper panel shows the schematic of the CUL4B deletions fused to the C terminus of GAL4 DNA-binding domain. The region fused to Gal4-DBD is graphically depicted. In the lower panel, Gal4 luciferase reporter assay was performed in HeLa-Gal4-Luc cells by transfection of Gal4-DBD-fusion deletion expression vectors. Relative activity is scored with −, +, ++, or +++ corresponding to the significance to facilitate the interpretation of the data.

increased H2AK119ub1 and H3K27me3 levels, and a decreased level of H3K4me3 (Figure 2D, left panel); whereas RING1B, a core component of the PRC1 complex, which was reported to contribute to the monoubiquitination of hisone H2AK119 (de Napoles et al., 2004), was dispensable in this case (Figure 2D, left panel). These experiments support an argument that CRL4B is functionally associated with H2AK119 monoubiquitination. Next, qChIP experiments were performed in HeLa-Gal4-Luc cells that were transfected with Gal4-CUL4B, Gal4-ΔDID, Gal4-ΔCullin, or control Gal4-DBD to investigate the recruitment of DDB1 and EZH2 to and the changes of the H2AK119ub1 and H3K27me3 on the Gal4 promoter. The results showed that, compared to Gal4-CUL4B, ΔDID mutant lost the ability to recruit endogenous DDB1 or EZH2 but still could bind to Gal4-UAS with the artificial recruitment by Gal4-DBD tag and conduct H2AK119 monoubiquitination through classical E1/E2 machinery, resulting in a marginal decrease in monoubiquitination on H2AK119 (Figure 2D, right panel). Although ΔCullin mutant retained the ability to recruit endogenous DDB1, it had no enzymatic activity on H2AK119 (Figure 2D, right panel), thus losing the ability to recruit EZH2 and trimethylate H3K27. These data are in agreement with a functional scheme of CRL4B in which CUL4B relies on its Cullin domain to recruit the enzymatic activity while it uses the DID domain to capture the substrates, favoring our argument that CRL4B promotes H2AK119 monoubiquitination.

To further validate this proposition, we performed in vitro ubiquitination assays. HeLa cells were transfected with FLAG-RING1B, FLAG-CUL4B, FLAG-ΔDID, FLAG-ΔCullin, or FLAG control vector. Cell lysates were affinity purified using FLAG M2 affinity gel, followed by in vitro ubiquitination assays. The results showed that H2AK119 is monoubiquitinated by CRL4B in an E1/E2- and E3-dependent manner (Figure 2E, left panel). It is interesting that, while ΔDID could weakly monoubiquitinate H2A on lysing 119, ΔCullin completely lost such enzymatic activity (Figure 2E, left panel). Co-IP experiments further confirmed that the DID domain is responsible for the formation of the CRL4B-PRC2 machinery, while Cullin domain is responsible for the binding of the ring finger protein ROC1 along with E1/E2/E3 (Figure 2E, right panel). As a positive control, affinity-purified FLAG-RING1B elution was more efficient in the catalysis of H2AK119ub1 than FLAG-CUL4B elution (Figure 2E, left panel). Experiments with H2A and its mutants, K118/R, K119/R, and K118/R+K119/R, indicated that the major ubiquitination site is K119, while residual ubiquitination is found at K118, as reported previously (Richly et al., 2010) (Figure 2F). It is known that Cullins do not directly bind to their substrates directly; they rely on adaptor/receptor proteins in their substrate recognition, such as F-box proteins for CUL1, BTB proteins for CUL3, and WD40 proteins for CUL4 (Zimmerman et al., 2010). To determine which WD40 protein is used for CUL4B to recognize H2AK119, we purified CRL4B subunits CUL4B, DDB1, and ROC1, respectively, from Sf9 insect cells. In vitro ubiquitination assays with the purified proteins showed that the WD40 protein RbAp46/48, not EED, acted as the substrate adaptor/receptor for CUL4B to recognize H2AK119 (Figure 2G, upper panels). Conversely, knocking down RbAp48 resulted in the decrease of H2AK119ub1 (Figure 2G, lower panels). Interestingly, we also found that the amount of chromatin-bound EZH2 was positively correlated with the expression level of CUL4B (Figure 2H) and that the transcription factors such as JARID2 and PHF1 that are essential for PRC2 recruitment (Sarma et al., 2008; Shen et al., 2009) could also interact with CRL4B (Figure S1), further supporting a functional connection between CRL4B and PRC2.

Depletion of CUL4B or Ablation of *Cul4b* Resulted in the Loss of H2AK119ub1 as well as H3K27me3

To further explore the functional relationship between CUL4B and PRC2, we next investigated whether CUL4B depletion would alter H2AK119ub1 and H3K27me3 in vivo. CUL4B-specific shRNA were tagged with enhanced green fluorescent protein (EGFP) and transfected into HeLa cells. Forty-eight hours posttransfection, cells were fixed and stained with antibodies recognizing CUL4B, H2AK119ub1, and H3K27me3. As shown in Figure 3A, although the expression of EZH2 was not affected by CUL4B knockdown, the signals representing H2AK119ub1 and H3K27me3 were significantly reduced in CUL4B-depleted cells, while H3K4me3 signals were slightly increased (marked by arrows). These observations were corroborated by western blotting (Figure 3B).

To further explore the importance of CUL4B in PRC2-mediated gene silencing in vivo, we examined the effect of CUL4B deficiency on the global level of H2AK119ub1 and

(C) Effect of depletion of DDB1, EZH2, BMI, or RING1B on CUL4B repressive activity. HeLa-Gal4-Luc cells were transiently transfected with DBD or DBD-CUL4B constructs along with the indicated shRNAs for 48 hr before luciferase assay. shSCR, control scrambled shRNA.
(D) CUL4B confers repressive activity through H2AK119ub1 catalysis and PRC2 recruitment. ChIP experiments were performed with transient transfection of Gal4-DBD, Gal4-CUL4B, or its deletion constructs. Chromatin was immunoprecipitated with antibodies against the proteins indicated at the bottom. ubH2A, H2AK119 monoubiquitination. DNA enrichment was analyzed at the Gal4 promoter and the results are presented as fold of enrichment over control. In (A–D), all the error bars represent mean ± SD of three independent experiments, and a two-tailed t test was performed (*$p < 0.05$; **$p < 0.01$; ***$p < 0.001$).
(E) The left panel shows in vitro ubiquitination analysis with recombinant CUL4B and CUL4B deletions incubated with different combinations of E1/E2 and recombinant H2A (substrate) along with ubiquitin and ATP. Reactants were subjected to IB with the indicated antibodies. A silver-stained gel on the bottom shows the quality of the isolated complexes. Arrows correspond to the overexpressed FLAG-tagged proteins. In the right panel, HeLa cells were transfected with FLAG-CUL4B or FLAG-tagged mutants, and whole-cell extracts were immunoprecipitated with anti-FLAG M2 resin followed by western blotting with antibodies against DDB1, ROC1, EZH2, SUZ12, RbAps, RING1B, or BMI.
(F) In vitro ubiquitination with recombinant His_6-tagged H2A and its mutants (Mut) purified from Sf9 insect cells. The recombinant substrates were stained by Coomassie blue and shown on the bottom. Exp, exposure.
(G) Upper panels show (left) Coomassie blue staining of CRL4B complex (containing CUL4B, DDB1, and ROC1) purified from Sf9 cells and (right) in vitro ubiquitination analysis using recombinant His_6-tagged CRL4B alone or with WD40 proteins RbAp48 or EED as substrate adaptor/receptors. His_6-tagged CUL4B served as a negative control. In the lower panels, western blotting analysis shows decrease in H2AK119ub1 in HeLa cells upon RbAp48 knockdown.
(H) CUL4B is required for the binding of EZH2 to chromatin and shares the same transcription factors with PRC2. Chromatin-bound fractions were prepared from HeLa cells and analyzed by immunoblotting with the indicated antibodies. Histone H3 served as a loading control.
See also Figure S1.

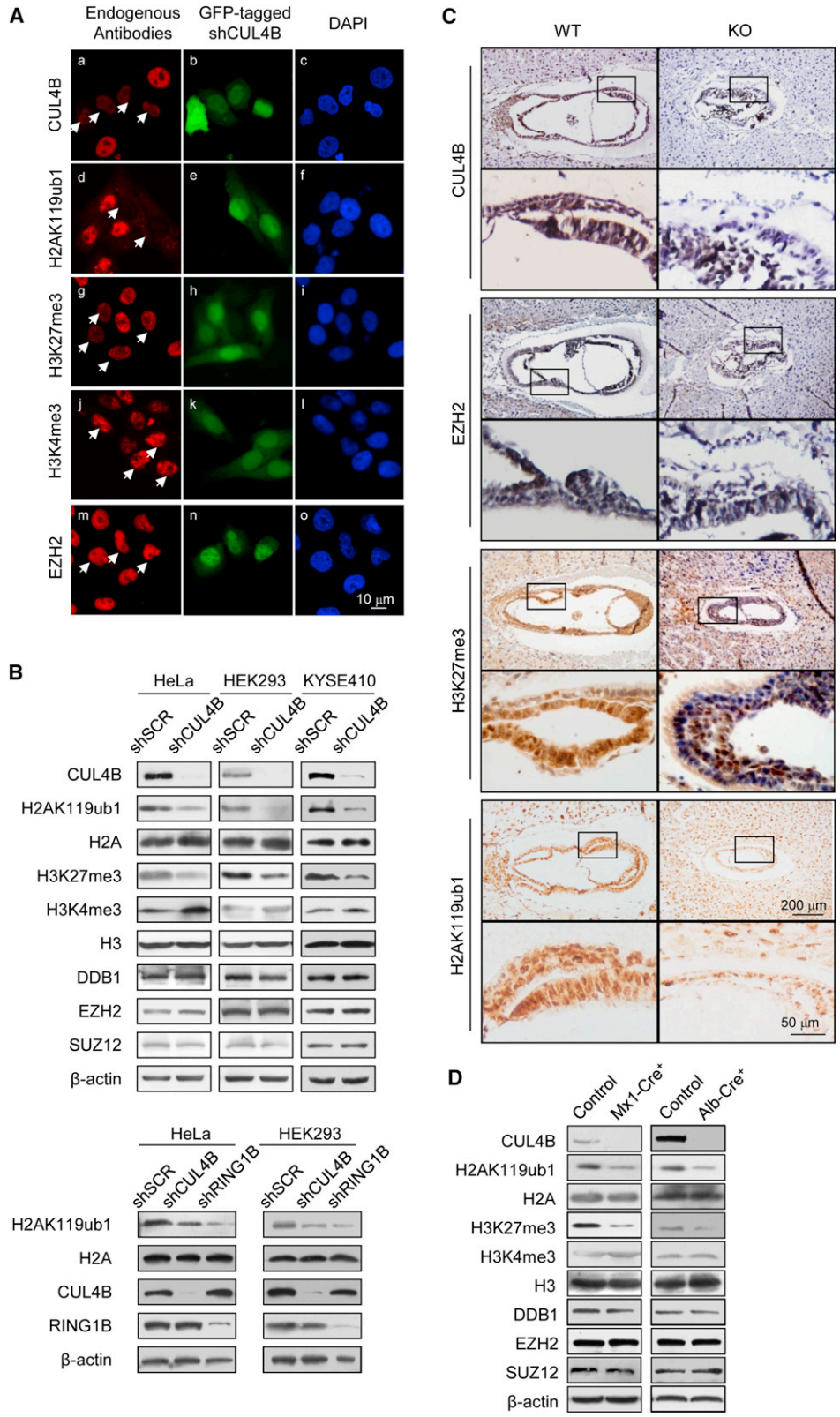

Figure 3. Knockdown of CUL4B or Ablation of Cul4b Resulted in Reduced H2AK119 Monoubiquitination and H3K27 Trimethylation

(A) HeLa cells were transiently transfected with EGFP-carrying CUL4B shRNA and stained with antibodies against CUL4B or EZH2 (red) or against H2AK119ub1, H3K27me3, or H3K4me3 (red). Nucleus was counterstained by DAPI. Significant decrease in H2AK119ub1 and H3K27me3 levels was marked with arrows.

H3K27me3 in *Cul4b* knockout mice. Since *Cul4b* null embryos usually die between 8.5 and 9.5 days postcoitum (dpc), we performed immunostaining on paraffin-embedded *Cul4b* WT and *Cul4b* null (KO) embryos at 7.5 dpc. Immunostaining revealed a significant decrease in H2AK119ub1 and H3K27me3 in the *Cul4b* null embryos, although the level of Ezh2 was comparable to that in WT E7.5 embryos (Figure 3C). These results support a notion that CUL4B is required for the monoubiquitination of H2AK119 and trimethylation of H3K27 during early embryonic development. In addition, examination of the global level of H2AK119ub1 and H3K27me3 in liver from liver-specific *Cul4b* knockout mice [Cul4b (loxp/Y)/Mx-1-Cre(+) and Cul4b (loxp/Y)/Alb-Cre(+)] by western blotting showed a significant reduction of both H2AK119ub1 and H3K27me3 in liver (Figure 3D), further supporting the arguments that CUL4B is required for the trimethylation of H3K27 and that CUL4B and PRC2 are functionally connected.

Genome-wide Identification of Transcription Targets for the CRL4B/PRC2 Complex

To further investigate the functional connection between CRL4B and PRC2 and to explore the biological significance of this connection, we next analyzed the genome-wide transcriptional targets of the CRL4B/PRC2 complex using the ChIP-on-chip (ChIP-on-chip) approach. In these experiments, ChIP experiments were conducted in KYSE410 cells with antibodies against CUL4B, EZH2, or BMI. Following ChIP, CUL4B-, EZH2-, and BMI-associated DNAs were amplified using nonbiased conditions, labeled, and hybridized to an oligonucleotide array covering 2.7 kb (−2.2 kb to +0.5 kb with respect to transcription start sites) of 18,028 annotated transcripts in the NCBI database with a false discovery rate less than 0.05 (GEO accession number: GSE41639). The data from CUL4B antibodies (1,463 genes) were then analyzed with the data from EZH2 (3,705 genes) and BMI antibodies (891 genes) for the identification of common targets, or cotargets (Figure 4A, left panel). The detailed results of the ChIP-on-chip experiments were summarized in Tables S2–S8. A total of 619 unique promoters were found to be cotargeted by CUL4B and EZH2, among which only 53 were overlapped with the 891 targets of BMI, indicating a predominant cooperation between PRC2 and CRL4B, at least in KYSE410 cells. The cotargets of CUL4B/CRL4B and EZH2/PRC2 were then classified into various cellular signaling pathways using Molecule Annotation System software (http://www.capitalbio.com/lifescience/informationsystems/2572.shtml), with a p value cutoff of 10^{-3} (Figure 4A, right panel). These signaling pathways include Wnt, MAPK, focal adhesion, IGF, and apoptosis that are critically involved in cell growth, survival, migration, and invasion. The genes in these pathways include, among others, *PTEN*, *SOCS1*, *AXIN2*, *SIAH1*, *RUXN1*, *FANCB*, *MCM8*, *COL4A1*, *IGFBP3*, and *CDKN2A (p16)*, that are known to be implicated in apoptosis and tumor suppression. Significantly, *FOXO3, E2F1, IGFBP3, p16,* and *TGFBI* have been shown to be transcriptionally repressed by PRC2 (Chen et al., 2009; Tan et al., 2007; Wu et al., 2010). Quantitative ChIP analysis in KYSE410 cells using specific antibodies against CUL4B, EZH2, RING1B, H2AK119ub1, and H3K27me3 on selected genes, including *PTEN*, *SOCS1*, *AXIN2*, *CXCR2*, *FOXO3*, *SIAH1*, *E2F1*, *RUXN1*, *FANCB*, *MCM8*, *NKD2*, *COL4A1*, *IGFBP3*, *p16*, *MLL3*, *CABLES2*, *RNH1*, and *TGFBI*, which represent each of the classified pathways, showed a strong correlation between CUL4B/H2AK119ub1 and EZH2/H3K27me3 enrichments, validating the ChIP-on-chip results (Figures 4B and 4C). Quantitative real-time PCR (qPCR) further showed that the transcription levels of most of the target genes significantly increased in KYSE410 cells upon knockdown of CUL4B or EZH2 (Figure S2).

We next investigated the effect of EZH2 depletion on the recruitment of CUL4B on endogenous target loci and vice versa. To this end, we established KYSE410 cells in which EZH2 expression was knocked down by its shRNA. In these cells, EZH2 was greatly reduced or barely detectable at the promoters of its target genes (Figure 4D, left panel). It is interesting that ChIP experiments with antibodies against CUL4B showed that EZH2 depletion resulted in only marginal or no effect on the recruitment of CUL4B on the target promoters (Figure 4D, right panel). However, in CUL4B-depleted KYSE410 cells, the recruitment of EZH2 to its target promoters was greatly reduced (Figure 4E), although the expression of EZH2 was not affected by CUL4B knockdown (see Figure 3B). In addition, consistent with our earlier observations, the levels of both H2AK119ub1 and H3K27me3 were markedly decreased at all the tested target genes upon CUL4B knockdown (Figure 4F). Collectively, these data suggest that CRL4B may function to promote the recruitment and/or the stabilization of PRC2 onto target promoters, supporting our aforementioned arguments that CUL4B and PRC2 are functionally connected and that CUL4B is required for the trimethylation of H3K27.

Regulation of *p16* and *PTEN* by the CLR4B/PRC2 Complex

Among the common target genes identified earlier, *p16* and *PTEN* are well-established tumor suppressor genes (Lowe and Sherr, 2003; Salmena et al., 2008). We thus further investigated the transcriptional regulation of *p16* and *PTEN* by CUL4B. As expected, CUL4B knockdown in KYSE410, HeLa, HEK293, MCF-7 (human breast adenocarcinoma cell line), and U2OS (human osteosarcoma cell line) led to increased expression of *p16* and *PTEN* at both the transcriptional level (Figure 5A, left panel) and the protein level (Figure 5A, right panel). Significantly, the levels of p16 and PTEN were also elevated in *Cul4b* null embryos (Figure 5B).

We then investigated the regulation of *p16* and *PTEN by* the CLR4B/PRC2 complex. ChIP assays in KYSE410 cells with

(B) Western blotting analysis showing decrease in H2AK119ub1 and H3K27me3 in HeLa, HEK293, and KYSE410 cells upon CUL4B knockdown (upper panels). RING1B knockdown served as a positive control (lower panels).
(C) Immunohistochemical staining of 7.5 dpc in utero embryo sections using antibodies recognizing mouse Cul4b, Ezh2, H3K27me3, and H2AK119ub1 in WT (left panels) and Cul4b KO (right panels) embryos. Different magnifications of the same embryos are presented.
(D) Western blotting analysis showing loss of H2AK119ub1 and H3K27me3 as well as Cul4b protein in conditional liver-specific *Cul4b* ablation mice. Histones H2A and H3 were used as loading controls.

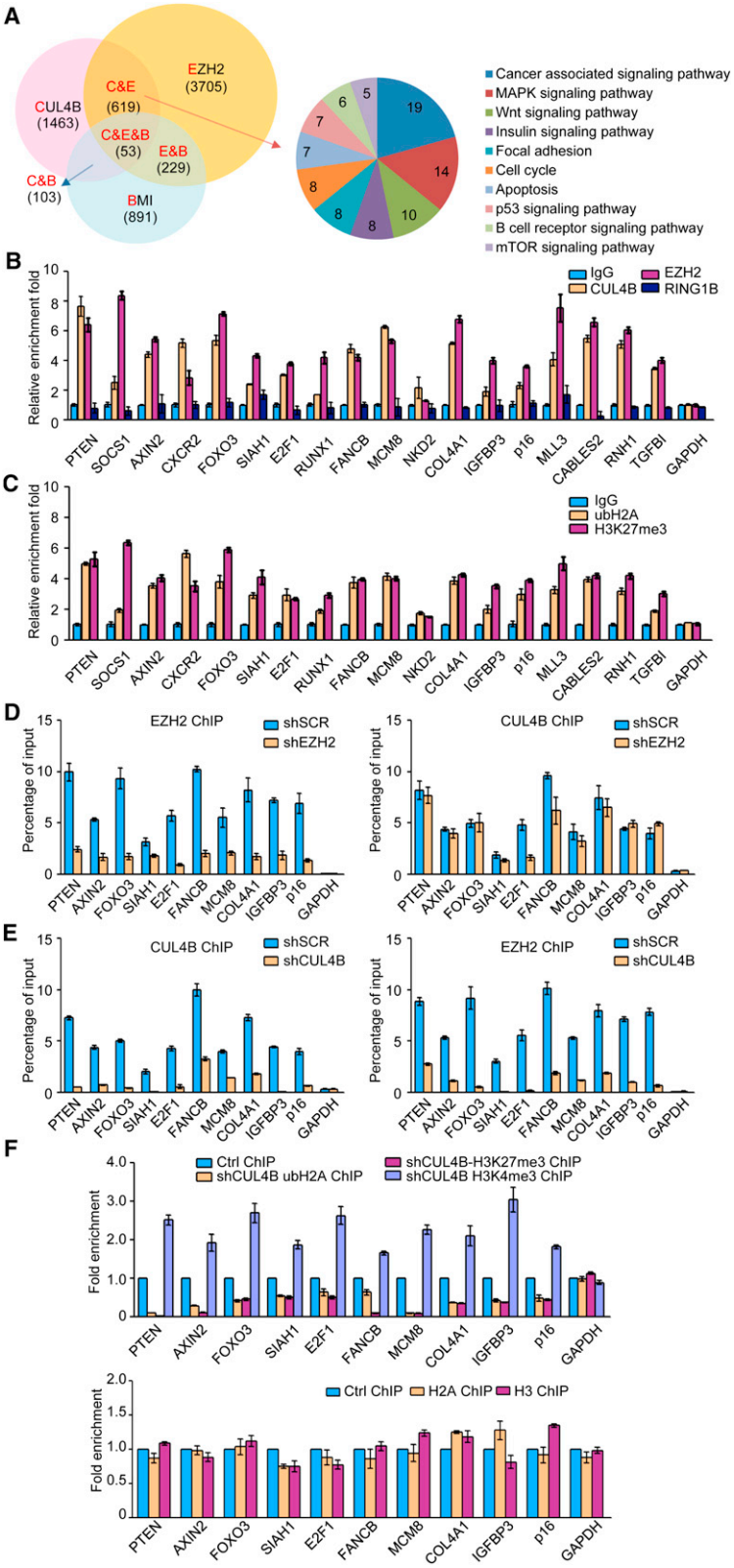

Figure 4. CUL4B/CRL4B and EZH2/PRC2 Co-Occupy Target Genes

(A) The left panel is a Venn diagram showing a statistically significant overlap between promoters bound by CUL4B, EZH2, and BMI in KYSE410 cells. The numbers represent the number of the promoters that were targeted by the indicated proteins. The right panel shows clustering of the 619 overlapping target genes of CUL4B and EZH2 into functional groups.

The detailed results of the ChIP-on-chip experiments are provided in Tables S2–S8.

(B and C) Verification of the ChIP-on-chip results by qChIP analysis of the indicated genes in KYSE410 cells.

(D–F) qChIP analysis of selected promoters in the KYSE410 cells after transfection with control shRNA or shRNAs targeting CUL4B or EZH2 using the indicated antibodies. Results are represented as fold change over control. GAPDH served as a negative control. Error bars represent mean ± SD of three independent experiments. See also Figure S2 and Tables S2–S8.

antibodies against CUL4B, DDB1, EZH2, SUZ12, or control mmnuoglobulin G (IgG) revealed that CRL4B and PRC2 co-occupied the promoters of *p16* and *PTEN* (Figure 5C, upper panels). To further test our proposition that CRL4B and PRC2 function in the same protein complex at *p16* and *PTEN* promoters, sequential ChIP or ChIP/Re-ChIP experiments (Wang et al., 2009) were performed. In these experiments, soluble chromatins were first immunoprecipitated with antibodies against CUL4B, DDB1, EZH2, SUZ12, or H2AK119ub1, while RING1B served as a negative control (Figure 5C, upper panels). The immunoprecipitates were subsequently reimmunoprecipitated with appropriate antibodies. The results showed that, in precipitates, the *p16* and *PTEN* promoters that were immunoprecipitated with antibodies against CUL4B could be reimmunoprecipitated with antibodies against DDB1, EZH2, SUZ12, or H2AK119ub1 (Figure 5C, lower panels). Similar results were obtained when initial ChIP was done with antibodies against DDB1, EZH2, SUZ12, or H2AK119ub1. Furthermore, profiling of the binding patterns of CUL4B, DDB1, EZH2, and SUZ12 by qChIP on a region of ~10 kb upstream and downstream of the transcription start sites of p16 or *PTEN* loci revealed a perfect overlap of the occupancy sites of these proteins, while RING1B/PRC1 binds mainly downstream from the transcription start sites (TSS) of *p16* locus, which is different from CRL4B/PRC2 (Figure 5D). Taken together, these results support the idea that CRL4B and PRC2 occupy the *p16* and *PTEN* promoters in one multiunit complex.

In order to determine a functional connection between CRL4B and PRC2 on *p16* and *PTEN* promoters, KYSE410 cells were transfected with shRNAs specifically against CUL4B, DDB1, EZH2, or SUZ12. Each of these shRNA led to a significant reduction in the expression of its target gene without causing detectable changes of the nontargeted genes (Figure 5E). qChIP analyses showed that knockdown of the expression of CUL4B or DDB1 led to a significant reduction of the binding of EZH2 and SUZ12 to the promoters of *p16* and

PTEN, whereas depletion of EZH2 or SUZ12 expression resulted in only a marginal decrease in the association of CUL4B and DDB1 with the promoters of *p16* and *PTEN* (Figure 5F), which was consistent with the results shown in Figures 4D and 4E. Notably, knockdown of either CUL4B or DDB1 led to a severe decrease in H3K27me3 at the promoters of *p16* and *PTEN*, whereas knockdown of either EZH2 or SUZ12 resulted in a limited reduction in the levels of H2AK119ub1 at the promoters of *p16* and *PTEN* (Figure 5F), suggesting that CRL4B-catalyzed H2AK119ub1 acts sequentially and coordinately with PRC2-mediated H3K27me3.

CUL4B Promotes Cell Proliferation and Invasion

Based on the role of PRC2 in cancer development and progression (Simon and Lange, 2008) and our observation that CRL4B and PRC2 are physically and functionally associated, we next investigated what role, if any, CUL4B plays in tumorigenesis. For this purpose, we first analyzed the effect of gain-of-function and loss-of-function of CUL4B and EZH2 on the cell cycle profile of KYSE410 cells by propidium iodide staining and flow cytometry. KYSE410 cells with stable CUL4B/EZH2 expression or with CUL4B/EZH2 knockdown were synchronized at the G_0/G_1 phases by serum starvation for 24 hr, followed by being released using normal growth media for another 12 hr. Compared with control, CUL4B or EZH2 overexpression was associated with a decreased cell population in G_1 and an increased cell population in the S phases, while KYSE410 cells exposed to CUL4B or EZH2 shRNA exhibited an increase in the proportion of cells in G_1 and a decrease in the proportion of cells in the S phases (Figure 6Aa). Growth curve assays showed that the S-phase accumulation by CUL4B overexpression was not due to S phase arrest (Figure 6Ab). The representative cytometric results from these experiments are shown in Figure S3. Furthermore, western blotting analysis showed that the expression level of CUL4B remained constant at different cell cycle stages, excluding the possibility that proliferation itself increases CUL4B expression (Figure 6B). The cyclin D1 level was low in quiescent cells, and it increased as cells progressed into G1, which served as a control protein (Koepp et al., 1999). These data indicate that CUL4B and EZH2 have similar effect on cell cycle progression in KYSE410 cells, consistent with the role of p16 and PTEN in arresting cells in the G_1 phase (Weng et al., 1999; Zhang et al., 1999). Moreover, colony formation assays further showed that CUL4B overexpression was associated with a marked increase in colony numbers, whereas CUL4B knockdown is associated with a significant decrease in colony numbers (Figure 6C). In addition, while overexpression of WT CUL4B resulted in 1.72-fold increase in colony number, overexpression of CUL4BΔCullin had a dominant negative effect on colony formation (Figure 6D, bars 1–3). Moreover, in agreement with the functional link between CUL4B and p16 described earlier, the positive effect of CUL4B overexpression on colony formation could be partially offset by introduction of exogenous p16 and the decrease in colony formation by CUL4B knockdown could be partially rescued by treatment of cells with p16 shRNA (Figure 6D). In addition, overexpression of CUL4B but knockdown of the expression of EZH2 resulted in a diminished effect of CUL4B on colony formation (Figure 6D, bars 6 and 7). Together, these experiments support a notion that CUL4B promotes esophagus carcinoma cell proliferation and it does so, at least in part, through cooperation with EZH2 and via repression of tumor suppressor p16.

As stated earlier, PRC2 has also been implicated in epithelial-to-mesenchymal transitions (EMT; Herranz et al., 2008). Thus, we next investigated whether CUL4B has a role in EMT and tumor metastasis. For this purpose, CUL4B was overexpressed in KYSE410 cells via stable transfection, and the impact of the gain-of-function of CUL4B on the invasive potential of these cells was assessed using transwell invasion assay. The results showed that, while overexpression of WT CUL4B resulted in more than 3-fold increase in cell invasion, overexpression of the Cullin domain-deleted CUL4B mutant had little effect (Figure 6E, bars 1–3). In addition, the increased invasiveness upon CUL4B overexpression was probably achieved through a concerted action by CRL4B and PRC2, as the effect of CUL4B overexpression was diminished when EZH2 was concomitantly knocked down (Figure 6E, bars 4 and 5). Moreover, the increase in invasiveness associated with CUL4B overexpression could be blocked by PTEN overexpression (Figure 6E, bars 6 and 7). Collectively, these results indicate that CUL4B promotes the invasive potential of KYSE410 cells, possibly by acting in conjunction with PRC2 and by repressing the expression of PTEN.

We next investigated the role of CUL4B in tumor development and progression in vivo by implanting KYSE410 and EC9706 cells that had been engineered to stably express CUL4B shRNA or control scrambled shRNA (shSCR) onto the subcutaneous sites of athymic BALB/c mice. Growth of the implanted tumors was monitored by measuring the tumor sizes every 4 days over a period of 4 weeks. The results showed that tumor growth was greatly suppressed by CUL4B knockdown, indicating that CUL4B had a significant effect on promoting the tumor growth (Figure 6F). Western blotting analysis confirmed the decrease in the levels of H2AK119ub1/H3K27me3 and the increases in the levels of p16 and PTEN proteins in the tumors with CUL4B knockdown (Figure 6G). Immunohistochemical staining for Ki-67, a well-documented marker for cellular proliferation, on serial xenograft tumor sections showed that, compared to the control, tumors with CUL4B knockdown exhibited significantly fewer Ki-67-positive nuclei (Figure 6H). Taken together, these experiments indicate that CUL4B promotes esophageal carcinoma cell proliferation, invasion, and tumorigenesis in vitro and in vivo.

The Expression of CUL4B Is Upregulated in Esophageal Carcinomas and Positively Correlated with Tumor Grade

To further define the role of CUL4B in tumorigenesis, we collected 182 esophageal carcinoma samples, 45 of them with paired adjacent normal tissues, from esophageal cancer patients and performed tissue microarrays by immunohistochemical staining. CUL4B was found to be significantly upregulated in tumors and its expression appeared to be positively correlated with histological grades (Figures 7A and 7B). In 12 of 14 selected paired samples of grade II cancers, the level of *CUL4B* mRNA was found to be higher in tumor tissue than in adjacent tissue, as measured by qPCR (Figure 7C, upper panel) and western blotting (Figure 7C, lower panel), and the levels of p16 and PTEN generally showed an inverse trend with that of CUL4B. Indeed, statistical analysis revealed a significant

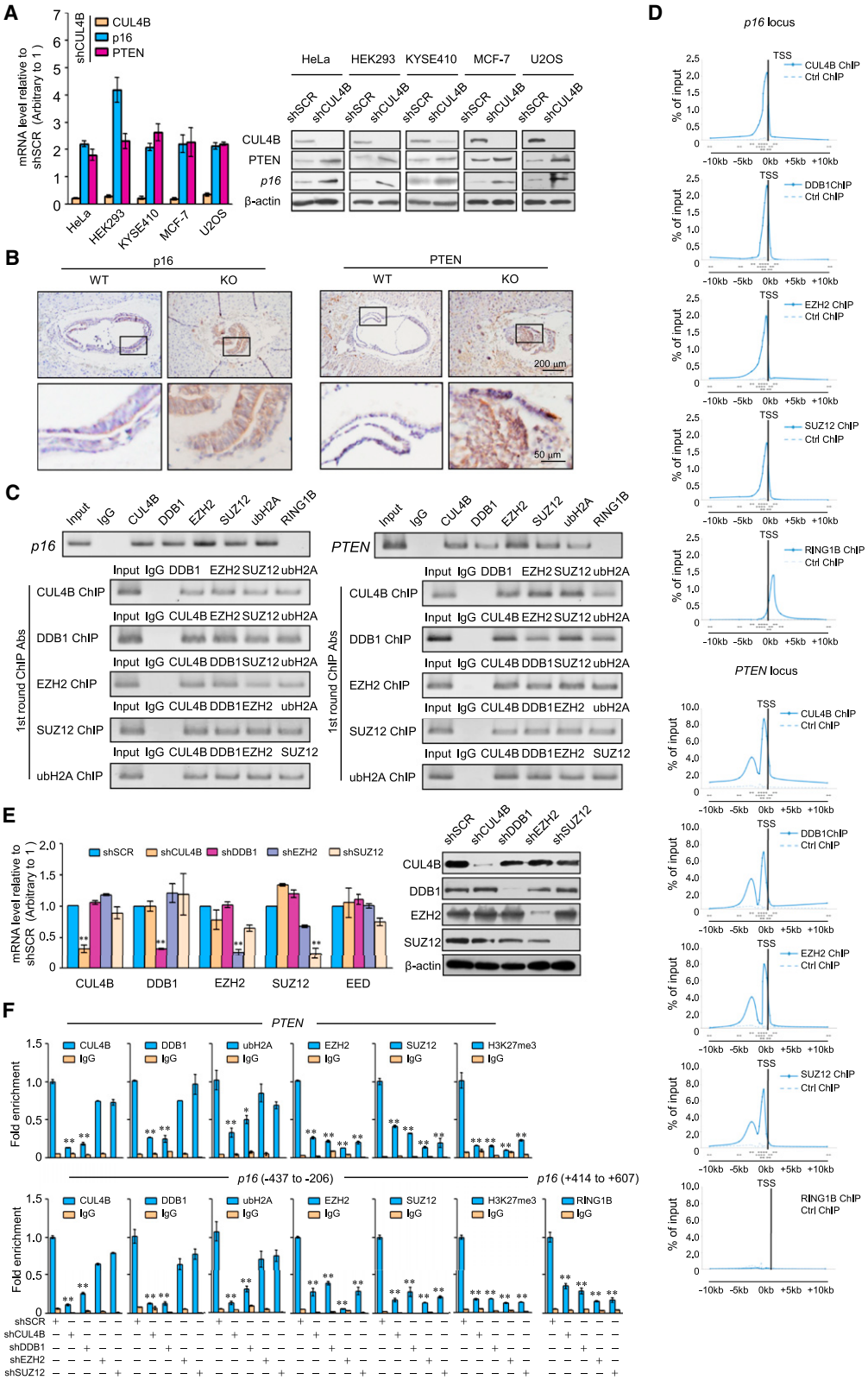

Figure 5. Tumor Suppressor Genes *p16* and *PTEN* Are Cotargeted by CLR4B and PRC2

(A) Clones in which CUL4B was stably knocked down were compared with the parental cell line with respect to the levels of mRNA (left panel) and protein (left panel) of p16 and PTEN in HeLa, HEK293, KYSE410, MCF-7, and U2OS cells. The mRNA levels were normalized to those of GADPH (left panel) and β-actin served as a loading control for the western blotting (right panel).

negative correlation when the relative expression levels of p16 and PTEN were plotted against that of CUL4B in 30 paired samples of grade II (Figure 7D). These data are consistent with a role of CUL4B in promoting carcinogenesis and support the observation that *p16* and *PTEN* are downstream targets of CUL4B.

To investigate whether the tumorigenic effect of CUL4B could be extended to a broader scope of cancers, we collected a series of carcinoma samples from esophageal, lung, gastric, colon, pancreatic, cervical, renal, and bladder cancer patients, with each type of carcinomas having at least three samples paired with adjacent normal tissues. Tissue microarray analysis by immunohistochemical staining showed a statistically significant upregulation of CUL4B expression in carcinomas from multiple tissues compared to the adjacent normal tissues, except for the carcinomas of urinary system (Figure 7E). Since EZH2 has also been reported to be overexpressed in various cancers (Simon and Lange, 2008), we also determined the expression profile of CUL4B and EZH2 using the human cancer survey qPCR gene expression panel (Origene) in tumors originated from breast, colon, kidney, lung, ovary, and thyroid (Figure 7F). The results showed that both CUL4B and EZH2 are overexpressed in all of these cancer groups compared with normal tissue controls except in the kidney. Moreover, the cancer survey cDNA array data also revealed a significant positive correlation between the expression of CUL4B or EZH2 and tumor grade, especially in breast and lung. The expression profiles of CUL4B and EZH2 were very similar. Taken together, these data support a role for CUL4B in promoting tumorigenesis and suggest that CUL4B could serve as a biomarker for cancer diagnosis and a potential target for cancer therapy.

DISCUSSION

Our data indicate CUL4B is a transcriptional corepressor that regulates transcription by recruiting PRC2. The CRL4B subunits do not contain chromatin-binding domains which could contribute to PRC2 recruitment (Figure 7Ga). Although RbAp46/48, two histone binding proteins, were identified to be the bridge molecules for interaction between CRL4B and PRC2, it is more probably that the role of RbAp46/48 in this CRL4B-PRC2 interaction is to recognize and bind histone H2A and H3 (Yoon et al., 2003), thus to further stabilize the binding of this multiunit complex to chromatin rather than to recruit PRC2. To date, PRC2 has been shown to mediate transcription repression by distinct sequence-specific transcription factors. Interestingly, we found that JARID2 and PHF1 could also physically interact with CRL4B in HeLa cells, suggesting that CRL4B and PRC2 may share similar transcription factors thus respond to same signal pathways. Of note, while DNA binding proteins are believed to be responsible for PRC2 recruitment in mammals, recent studies indicated that long noncoding RNA, such as XIST, KCNQ1OT1, and HOTAIR, could also be involved in this process (Maenner et al., 2010; Pandey et al., 2008; Tsai et al., 2010). It is intriguing that Pcu4 and Rik1, the fission yeast homologs of the CUL4 and DDB1, were reported to be involved in noncoding RNA transcription (Hong et al., 2005; Li et al., 2008) (Figure 7Gb). Clearly, future investigations are needed to explore the scope and the variety of the functionality of the CRL4B/PRC2 complex and to determine whether this functionality involves additional elements.

Recent studies showed that there are genes targeted by PRC2 without PRC1, and vice versa (Ku et al., 2008; Tavares et al., 2012). Our findings suggest that CRL4B may function as an alternate histone modification enzyme responsible for H2AK119ub1, providing a molecular basis for the interplay of H2AK119ub1 and H3K27me3 in chromatin remodeling. The replacement of PRC1 by CRL4B could also explain why PRC1 and PRC2 are uncoupled in some instances.

The regulation of *p16* and *PTEN* by CRL4B/PRC2 may have significant physiological implications. In addition to the propositions that CRL4 possibly promotes tumorigenesis through degradation of p53 as well as several cyclin-dependent kinase inhibitors (Banks et al., 2006; Nishitani et al., 2008), our findings add another element to the understanding of the oncogenic potential of CRL4. In this regard, it is interesting to note that CUL4A-DDB1 is reported to cooperate with the MLL1 complex in mediating oncogene-induced p16 activation (Kotake et al., 2009). It appears that CUL4A and CUL4B may have opposite effects on p16 expression and function in a competitive manner. The derepressive effect of CUL4B's loss-of-function combined with the activating effect of CUL4A's gain-of-function resulted in further p16 activation in HeLa and HEK293 cells, in which p16 is highly expressed due to the inactivation of Rb pathway (Kotake et al., 2007). Future studies would clarify whether CRL4 complexes could exert opposite activities depending on the different Cullin member in the complex.

In summary, our study revealed that CRL4B regulates transcription by monoubiquitinating H2AK119 and by coordinating/facilitating PRC2-catalyzed H3K27me3, thus providing a molecular basis for the interplay between histone ubiquitination and methylation in chromatin remodeling. Our data indicate that CUL4B functions as a transcription corepressor and a potential oncogene, supporting the pursuit of CUL4B as a target for cancer therapy.

(B) Different magnifications of immunohistochemical staining using antibodies recognizing mouse p16 and PTEN in WT (left panels) and Cul4B KO (right panels) 7.5 dpc embryos.

(C) The CRL4B and PRC2 complexes exist in the same protein complex on the p16 and PTEN promoters. ChIP and Re-ChIP experiments were performed in KYSE410 cells with the indicated antibodies.

(D) ChIP analysis of the recruitment of CUL4B, DDB1, EZH2, SUZ12, and RING1B on *PTEN* and *p16* gene loci in KYSE410 cells. Rabbit normal IgG served as negative control. ChIP enrichments are presented as percentage of bound/input signal. The position of the qPCR amplicons (arrows) relative to the genes are denoted as black boxes. TSS (dashed line) are also presented in the figure.

(E) The knockdown efficiencies of CUL4B, DDB1, EZH2, and SUZ12 were confirmed by qPCR (left panel) or western blotting (right panel).

(F) qChIP analysis of the recruitment of the indicated proteins on *p16* and *PTEN* promoters in KYSE410 cells after transfection with control shRNA or shRNAs targeting CUL4B, DDB1, EZH2, or SUZ12. RING1B ChIP was also performed on the binding peak shown in Figure 5D. Purified rabbit IgG was used as a negative control. Error bars represent mean ± SD of three independent experiments. *$p < 0.05$ and **$p < 0.01$ (two-tailed unpaired t test).

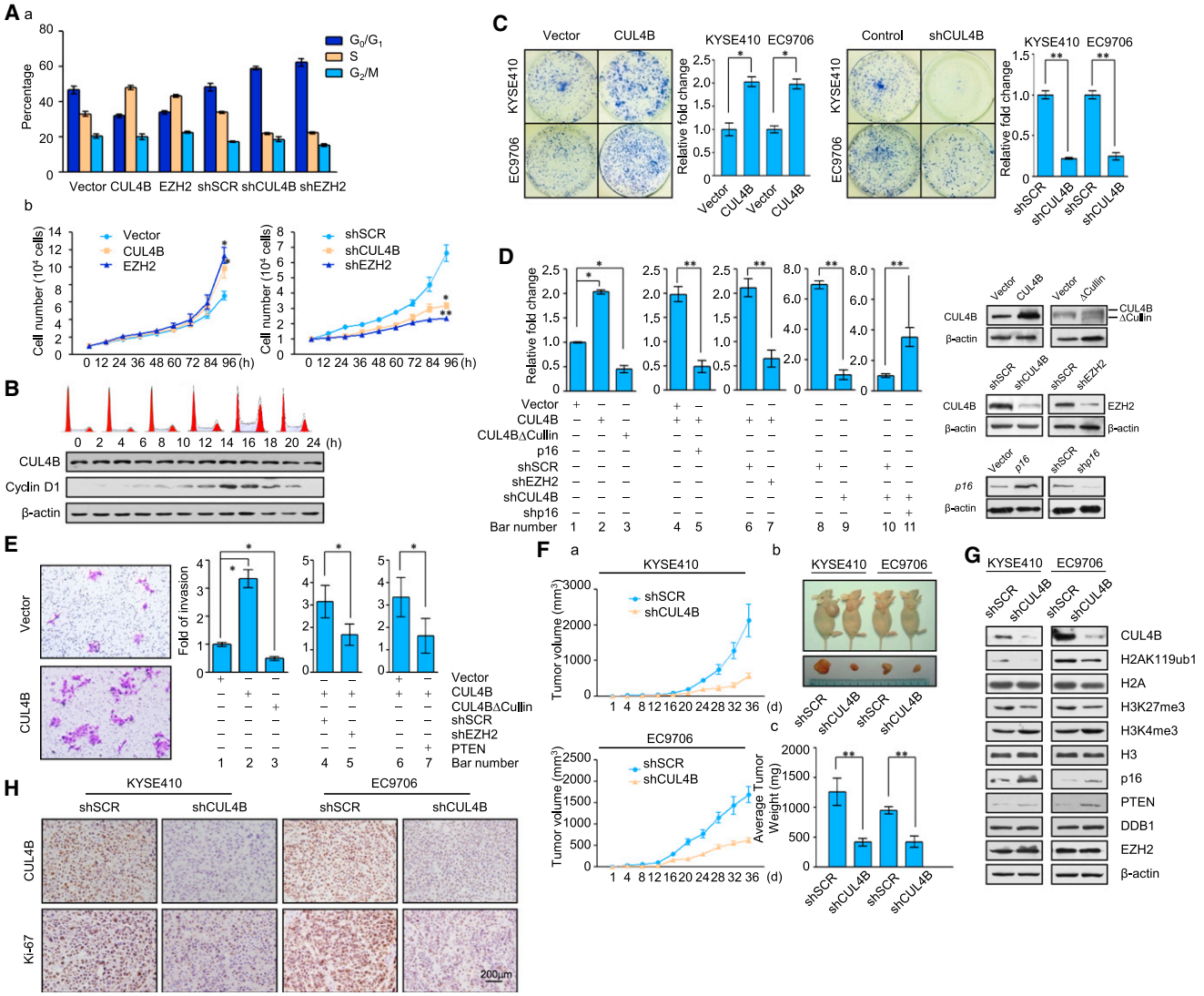

Figure 6. CUL4B Promotes Esophageal Carcinogenesis In Vitro and In Vivo

(A) CUL4B promotes cellular proliferation. KYSE410 cells stably expressing CUL4B/EZH2 or stably transfected with CUL4B/EZH2 shRNA were subjected to cell cycle analysis by flow cytometry (a) and growth curve assay (b). Error bars represent mean ± SD of three independent experiments.

(B) CUL4B remained unchanged throughout the cell cycle in KYSE410 cells. The cells were synchronized at the G0/G1 phases by serum starvation for 24 hr, followed by releasing into normal growth media. Propidium iodide FACS analysis is presented at the top of the panel.

(C) CUL4B enhances the colony-forming efficiency of esophageal cancer cells. KYSE410 cells and EC9706 cells stably expressing corresponding plasmids or shRNA vectors were maintained in culture media for 14 days under the presence of 1 mg/ml G418 prior to being stained with crystal violet.

(D) Enhancement in colony-forming efficiency by CUL4B is p16 and EZH2-dependent. KYSE410 cells were transiently transfected with empty vector, CUL4B expression vector, CUL4ΔCullin expression vector, p16 expression vector, control shRNA, EZH2 shRNA, CUL4B shRNA and p16 shRNA as indicated and maintained in culture media for 14 days under the presence of 1 mg/ml G418 and stained with crystal violet. The protein expression in these experiments was examined by western blotting using antibodies against the indicated proteins.

(E) CUL4B enhances the invasiveness of esophageal cancer cells. KYSE410 cell were transiently transfected with empty vector, CUL4B expression vector, CUL4ΔCullin expression vector, PTEN expression vector, control shRNA, or EZH2 shRNA as indicated and maintained in culture media for 14 days under the presence of 1 mg/ml G418 and assayed for transwell assay. In each experiment in (C–E), at least six randomly selected view fields (40× magnifications) were scored. The number of colonies or transwelled cells in each condition was counted and expressed as mean ± SD from triplicate experiments.

(F) CUL4B promotes esophageal tumorigenesis. KYSE410 and EC9706 cells stably expressing CUL4B shRNA or shRNA were transplanted into athymic mice. Tumors were measured every 4 days using a vernier calliper, and the volume was calculated according to the formula: 1/6 × length × width^2. The growth curves of tumors (a), representative images of tumor-bearing mice (b), and their tumors and the average tumor mass of each group (c) are shown. Each point represents the mean ± SEM. *$p < 0.05$ and **$p < 0.01$ (two-tailed unpaired t test).

(G) Western blotting analysis showing loss of H2AK119ub1 and H3K27me3 as well as increase in p16 and PTEN proteins in the tumors.

(H) CUL4B promotes esophageal tumorigenesis through accelerating cell proliferation. Immunohistochemical staining was used, using antibodies against mouse CUL4B and Ki-67 on xenograft tumor sections.

See also Figure S3.

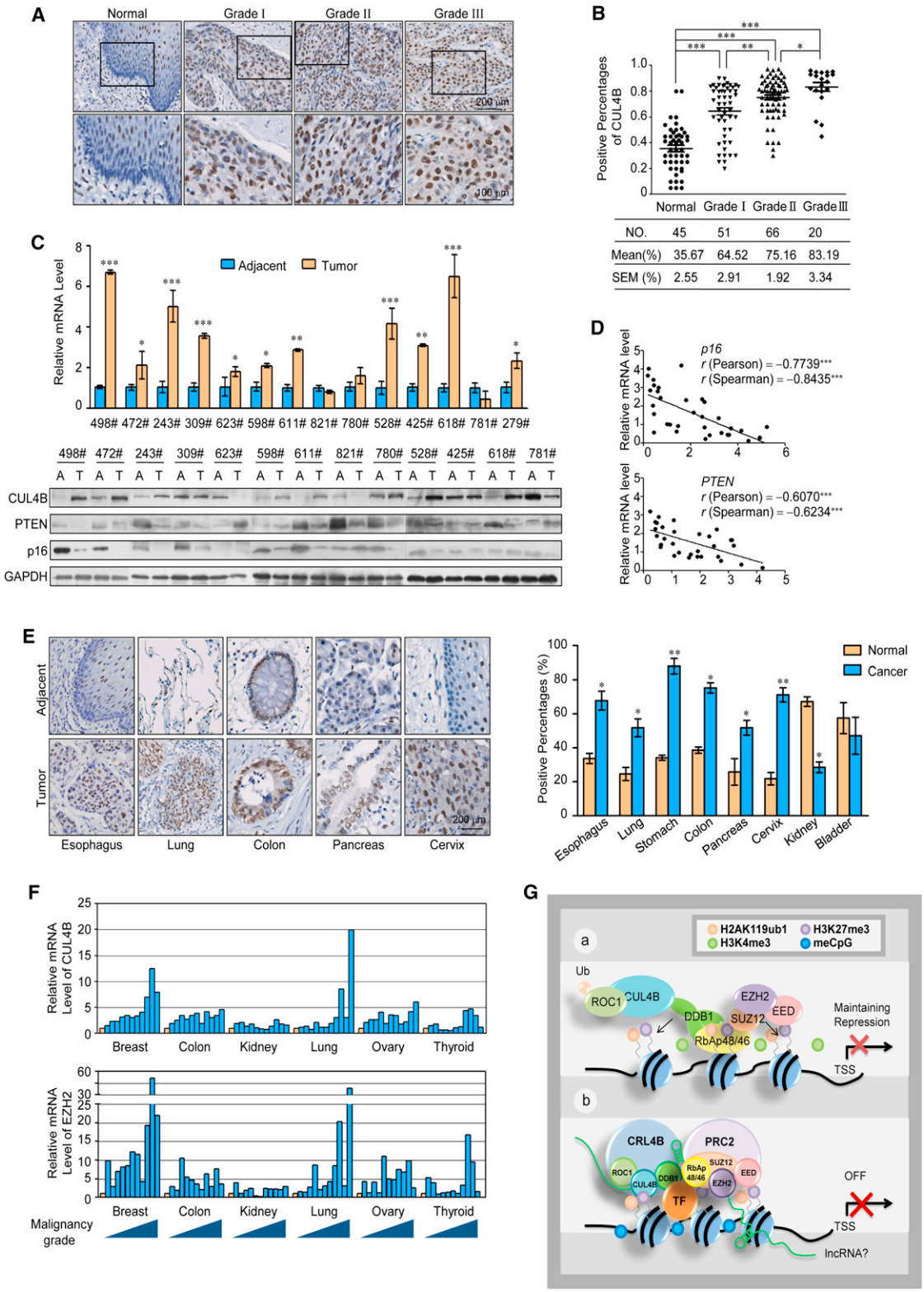

Figure 7. CUL4B Is a Potential Cancer Biomarker

(A) Immunohistochemical staining of CUL4B in normal esophageal tissue and esophageal carcinomas (histological grades I, II, and III). (B) The positively stained nuclei (in percentages) in grouped samples were analyzed by two-tailed unpaired t test (*$p < 0.05$; **$p < 0.01$; ***$p < 0.001$).

(C) The expression of CUL4B mRNA and protein is upregulated in esophageal carcinomas. Total RNAs and proteins in paired samples of esophageal carcinomas versus adjacent normal esophageal tissues were extracted, and the expression of CUL4B was measured by qPCR and western blotting. mRNA levels were

EXPERIMENTAL PROCEDURES

Tumor Xenografts

KYSE410 and EC9706 esophageal cancer cells stably transfected with CUL4B shRNA or scrambled control shRNA were collected, and 2 × 10^6 viable cells in 100 μl PBS were injected subcutaneously into 6- to 8-week-old BALB/c nude mice (Vital River Laboratories, Beijing, China). Eight animals per group (male = 4 and female = 4) were used in each experiment. Tumors were measured every 4 days using a vernier caliper, and the volume was calculated according to the formula: 1/6 × length × square width. All studies were approved by the Animal Care Committee of Shandong University Medical School.

Tissue Specimen and Immunohistochemistry

Esophageal carcinoma tissues were obtained from Qilu Hospital of Shandong University. Samples were frozen in liquid nitrogen immediately after surgical removal and maintained at −80°C until analyzed. Samples were fixed in 4% paraformaldehyde (Sigma-Aldrich) at 4°C overnight, and then embedded in paraffin, sectioned at 8 μm onto Superfrost-Plus Slides, and processed per standard protocols using DAB staining. All human tissue was collected using protocols approved by the Ethics Committee of Shandong University Medical School, and informed consent was obtained from all patients.

ACCESSION NUMBERS

ChIP-on-chip information was deposited at the Gene Expression Omnibus database (http://www.ncbi.nlm.nih.gov/geo/) with the accession number GSE41639.

SUPPLEMENTAL INFORMATION

Supplemental Information includes three figures, eight tables, and Supplemental Experimental Procedures and can be found in this article online at http://dx.doi.org/10.1016/j.ccr.2012.10.024.

ACKNOWLEDGMENTS

This work was supported by the National Natural Science Foundation of China and Ministry of Science and Technology of China (Grant 30830065 to Y.G. and C.S.; Grant 2011CB966201 to Y.W. and C.S.; Grants 90919053 and 31171240 to Y.W.; Grant 81021001 to Y.G. and C.S.; and Grant 2013CB910900 to Y.G.).

Received: May 9, 2012
Revised: August 19, 2012
Accepted: October 31, 2012
Published: December 10, 2012

REFERENCES

Baarends, W.M., Wassenaar, E., van der Laan, R., Hoogerbrugge, J., Sleddens-Linkels, E., Hoeijmakers, J.H., de Boer, P., and Grootegoed, J.A. (2005). Silencing of unpaired chromatin and histone H2A ubiquitination in mammalian meiosis. Mol. Cell. Biol. *25*, 1041–1053.

Banks, D., Wu, M., Higa, L.A., Gavrilova, N., Quan, J., Ye, T., Kobayashi, R., Sun, H., and Zhang, H. (2006). L2DTL/CDT2 and PCNA interact with p53 and regulate p53 polyubiquitination and protein stability through MDM2 and CUL4A/DDB1 complexes. Cell Cycle *5*, 1719–1729.

Cao, R., Tsukada, Y., and Zhang, Y. (2005). Role of Bmi-1 and Ring1A in H2A ubiquitylation and Hox gene silencing. Mol. Cell *20*, 845–854.

Chen, H., Gu, X., Su, I.H., Bottino, R., Contreras, J.L., Tarakhovsky, A., and Kim, S.K. (2009). Polycomb protein Ezh2 regulates pancreatic beta-cell Ink4a/Arf expression and regeneration in diabetes mellitus. Genes Dev. *23*, 975–985.

de Napoles, M., Mermoud, J.E., Wakao, R., Tang, Y.A., Endoh, M., Appanah, R., Nesterova, T.B., Silva, J., Otte, A.P., Vidal, M., et al. (2004). Polycomb group proteins Ring1A/B link ubiquitylation of histone H2A to heritable gene silencing and X inactivation. Dev. Cell *7*, 663–676.

Groisman, R., Polanowska, J., Kuraoka, I., Sawada, J., Saijo, M., Drapkin, R., Kisselev, A.F., Tanaka, K., and Nakatani, Y. (2003). The ubiquitin ligase activity in the DDB2 and CSA complexes is differentially regulated by the COP9 signalosome in response to DNA damage. Cell *113*, 357–367.

He, Y.J., McCall, C.M., Hu, J., Zeng, Y., and Xiong, Y. (2006). DDB1 functions as a linker to recruit receptor WD40 proteins to CUL4-ROC1 ubiquitin ligases. Genes Dev. *20*, 2949–2954.

Herranz, N., Pasini, D., Díaz, V.M., Francí, C., Gutierrez, A., Dave, N., Escrivà, M., Hernandez-Muñoz, I., Di Croce, L., Helin, K., et al. (2008). Polycomb complex 2 is required for E-cadherin repression by the Snail1 transcription factor. Mol. Cell. Biol. *28*, 4772–4781.

Higa, L.A., Wu, M., Ye, T., Kobayashi, R., Sun, H., and Zhang, H. (2006). CUL4-DDB1 ubiquitin ligase interacts with multiple WD40-repeat proteins and regulates histone methylation. Nat. Cell Biol. *8*, 1277–1283.

Hong, E.J., Villén, J., Gerace, E.L., Gygi, S.P., and Moazed, D. (2005). A cullin E3 ubiquitin ligase complex associates with Rik1 and the Clr4 histone H3-K9 methyltransferase and is required for RNAi-mediated heterochromatin formation. RNA Biol. *2*, 106–111.

Jackson, S., and Xiong, Y. (2009). CRL4s: the CUL4-RING E3 ubiquitin ligases. Trends Biochem. Sci. *34*, 562–570.

Jiang, B., Zhao, W., Yuan, J., Qian, Y., Sun, W., Zou, Y., Guo, C., Chen, B., Shao, C., and Gong, Y. (2012). Lack of Cul4b, an E3 ubiquitin ligase component, leads to embryonic lethality and abnormal placental development. PLoS ONE *7*, e37070.

Koepp, D.M., Harper, J.W., and Elledge, S.J. (1999). How the cyclin became a cyclin: regulated proteolysis in the cell cycle. Cell *97*, 431–434.

Kotake, Y., Cao, R., Viatour, P., Sage, J., Zhang, Y., and Xiong, Y. (2007). pRB family proteins are required for H3K27 trimethylation and Polycomb repression complexes binding to and silencing p16INK4alpha tumor suppressor gene. Genes Dev. *21*, 49–54.

Kotake, Y., Zeng, Y., and Xiong, Y. (2009). DDB1-CUL4 and MLL1 mediate oncogene-induced p16INK4a activation. Cancer Res. *69*, 1809–1814.

Kouzarides, T. (2007). Chromatin modifications and their function. Cell *128*, 693–705.

Ku, M., Koche, R.P., Rheinbay, E., Mendenhall, E.M., Endoh, M., Mikkelsen, T.S., Presser, A., Nusbaum, C., Xie, X., Chi, A.S., et al. (2008). Genomewide

normalized to those of GADPH (upper panel) and β-actin served as a loading control for the western blotting (lower panel). Each bar represents the mean ± SD for triplicate experiments (*$p < 0.05$ and ** < 0.01).

(D) CUL4B mRNA level is negatively correlated with the level of p16 and PTEN mRNA. The relative level of CUL4B expression was plotted against the relative level of p16 (upper panel) and PTEN (lower panel) expression (***$p < 0.001$).

(E) CUL4B is unregulated in multiple carcinomas. Immunohistochemical staining of CUL4B in paired samples of esophagus, lung, pancreas, stomach, colon, cervix, kidney, and bladder carcinoma versus adjacent normal tissues. Representative images of 200-fold magnifications of each type of paired tumor section are presented. Each bar represents the mean ± SEM for triplicate experiments (*$p < 0.05$ and ** < 0.01).

(F) Transcript levels of CUL4B and EZH2 are significantly higher in multiple malignant tumor tissues. Relative levels of CUL4B and EZH2 transcripts were normalized to that of GAPDH and calibrated to the mean mRNA level (arbitrary value of 1) in normal tissue (yellow bars). The fold increase in gene expression relative to the mean value for each disease sample is indicated.

(G) Graphic model as discussed in the text. DNA (black line); nucleosomes with single N terminus of H3 and C terminus of H2A (blue ball); transcription factors (TF, orange ball); long noncoding RNA (lncRNA, green line).

analysis of PRC1 and PRC2 occupancy identifies two classes of bivalent domains. PLoS Genet. *4*, e1000242.

Li, F., Huarte, M., Zaratiegui, M., Vaughn, M.W., Shi, Y., Martienssen, R., and Cande, W.Z. (2008). Lid2 is required for coordinating H3K4 and H3K9 methylation of heterochromatin and euchromatin. Cell *135*, 272–283.

Lowe, S.W., and Sherr, C.J. (2003). Tumor suppression by Ink4a-Arf: progress and puzzles. Curr. Opin. Genet. Dev. *13*, 77–83.

Maenner, S., Blaud, M., Fouillen, L., Savoye, A., Marchand, V., Dubois, A., Sanglier-Cianférani, S., Van Dorsselaer, A., Clerc, P., Avner, P., et al. (2010). 2-D structure of the A region of Xist RNA and its implication for PRC2 association. PLoS Biol. *8*, e1000276.

Müller, J., and Verrijzer, P. (2009). Biochemical mechanisms of gene regulation by polycomb group protein complexes. Curr. Opin. Genet. Dev. *19*, 150–158.

Nakagawa, T., and Xiong, Y. (2011). X-linked mental retardation gene CUL4B targets ubiquitylation of H3K4 methyltransferase component WDR5 and regulates neuronal gene expression. Mol. Cell *43*, 381–391.

Nishitani, H., Shiomi, Y., Iida, H., Michishita, M., Takami, T., and Tsurimoto, T. (2008). CDK inhibitor p21 is degraded by a proliferating cell nuclear antigen-coupled Cul4-DDB1Cdt2 pathway during S phase and after UV irradiation. J. Biol. Chem. *283*, 29045–29052.

Pandey, R.R., Mondal, T., Mohammad, F., Enroth, S., Redrup, L., Komorowski, J., Nagano, T., Mancini-Dinardo, D., and Kanduri, C. (2008). Kcnq1ot1 antisense noncoding RNA mediates lineage-specific transcriptional silencing through chromatin-level regulation. Mol. Cell *32*, 232–246.

Richly, H., Rocha-Viegas, L., Ribeiro, J.D., Demajo, S., Gundem, G., Lopez-Bigas, N., Nakagawa, T., Rospert, S., Ito, T., and Di Croce, L. (2010). Transcriptional activation of polycomb-repressed genes by ZRF1. Nature *468*, 1124–1128.

Salmena, L., Carracedo, A., and Pandolfi, P.P. (2008). Tenets of PTEN tumor suppression. Cell *133*, 403–414.

Sarma, K., Margueron, R., Ivanov, A., Pirrotta, V., and Reinberg, D. (2008). Ezh2 requires PHF1 to efficiently catalyze H3 lysine 27 trimethylation in vivo. Mol. Cell. Biol. *28*, 2718–2731.

Schuettengruber, B., Chourrout, D., Vervoort, M., Leblanc, B., and Cavalli, G. (2007). Genome regulation by polycomb and trithorax proteins. Cell *128*, 735–745.

Shen, X., Kim, W., Fujiwara, Y., Simon, M.D., Liu, Y., Mysliwiec, M.R., Yuan, G.C., Lee, Y., and Orkin, S.H. (2009). Jumonji modulates polycomb activity and self-renewal versus differentiation of stem cells. Cell *139*, 1303–1314.

Simon, J.A., and Lange, C.A. (2008). Roles of the EZH2 histone methyltransferase in cancer epigenetics. Mutat. Res. *647*, 21–29.

Simon, J.A., and Kingston, R.E. (2009). Mechanisms of polycomb gene silencing: knowns and unknowns. Nat. Rev. Mol. Cell Biol. *10*, 697–708.

Tan, J., Yang, X., Zhuang, L., Jiang, X., Chen, W., Lee, P.L., Karuturi, R.K., Tan, P.B., Liu, E.T., and Yu, Q. (2007). Pharmacologic disruption of Polycomb-repressive complex 2-mediated gene repression selectively induces apoptosis in cancer cells. Genes Dev. *21*, 1050–1063.

Tavares, L., Dimitrova, E., Oxley, D., Webster, J., Poot, R., Demmers, J., Bezstarosti, K., Taylor, S., Ura, H., Koide, H., et al. (2012). RYBP-PRC1 complexes mediate H2A ubiquitylation at polycomb target sites independently of PRC2 and H3K27me3. Cell *148*, 664–678.

Tsai, M.C., Manor, O., Wan, Y., Mosammaparast, N., Wang, J.K., Lan, F., Shi, Y., Segal, E., and Chang, H.Y. (2010). Long noncoding RNA as modular scaffold of histone modification complexes. Science *329*, 689–693.

Wang, H., Wang, L., Erdjument-Bromage, H., Vidal, M., Tempst, P., Jones, R.S., and Zhang, Y. (2004). Role of histone H2A ubiquitination in Polycomb silencing. Nature *431*, 873–878.

Wang, Y., Zhang, H., Chen, Y., Sun, Y., Yang, F., Yu, W., Liang, J., Sun, L., Yang, X., Shi, L., et al. (2009). LSD1 is a subunit of the NuRD complex and targets the metastasis programs in breast cancer. Cell *138*, 660–672.

Weng, L.P., Smith, W.M., Dahia, P.L., Ziebold, U., Gil, E., Lees, J.A., and Eng, C. (1999). PTEN suppresses breast cancer cell growth by phosphatase activity-dependent G1 arrest followed by cell death. Cancer Res. *59*, 5808–5814.

Wu, Z.L., Zheng, S.S., Li, Z.M., Qiao, Y.Y., Aau, M.Y., and Yu, Q. (2010). Polycomb protein EZH2 regulates E2F1-dependent apoptosis through epigenetically modulating Bim expression. Cell Death Differ. *17*, 801–810.

Yoon, H.G., Chan, D.W., Huang, Z.Q., Li, J., Fondell, J.D., Qin, J., and Wong, J. (2003). Purification and functional characterization of the human N-CoR complex: the roles of HDAC3, TBL1 and TBLR1. EMBO J. *22*, 1336–1346.

Zhang, H.S., Postigo, A.A., and Dean, D.C. (1999). Active transcriptional repression by the Rb-E2F complex mediates G1 arrest triggered by p16INK4a, TGFbeta, and contact inhibition. Cell *97*, 53–61.

Zimmerman, E.S., Schulman, B.A., and Zheng, N. (2010). Structural assembly of cullin-RING ubiquitin ligase complexes. Curr. Opin. Struct. Biol. *20*, 714–721.

Zou, Y., Liu, Q., Chen, B., Zhang, X., Guo, C., Zhou, H., Li, J., Gao, G., Guo, Y., Yan, C., et al. (2007). Mutation in CUL4B, which encodes a member of cullin-RING ubiquitin ligase complex, causes X-linked mental retardation. Am. J. Hum. Genet. *80*, 561–566.

Zou, Y., Mi, J., Cui, J., Lu, D., Zhang, X., Guo, C., Gao, G., Liu, Q., Chen, B., Shao, C., and Gong, Y. (2009). Characterization of nuclear localization signal in the N terminus of CUL4B and its essential role in cyclin E degradation and cell cycle progression. J. Biol. Chem. *284*, 33320–33332.